Anal Bioanal Chem (2010) 398:1633–1641
DOI 10.1007/s00216-010-4051-7

ORIGINAL PAPER

In situ evaluation of chromium–DNA damage using a DNA-electrochemical biosensor

S. Carlos B. Oliveira · A. M. Oliveira-Brett

Received: 15 March 2010 / Revised: 19 July 2010 / Accepted: 20 July 2010 / Published online: 5 August 2010

Abstract The *in situ* evaluation of the direct interaction of chromium species with double-stranded DNA (dsDNA) was studied using differential pulse voltammetry at a glassy carbon electrode. The DNA damage was electrochemically detected following the changes in the oxidation peaks of guanosine and adenosine bases. The results obtained revealed the interaction with dsDNA of the Cr(IV) and Cr(V) reactive intermediates of Cr(III) oxidation by O_2 dissolved in the solution bound to dsDNA. This interaction leads to different modifications and causes oxidative damage in the B-DNA structure. Using polyhomonucleotides of guanine and adenine, it was shown that the interaction between reactive intermediates Cr(IV) and Cr(V)–DNA causes oxidative damage and preferentially takes place at guanine-rich segments, leading to the formation of 8-oxoguanine, the oxidation product of guanine residues and a biomarker of DNA oxidative damage. The interaction of Cr(VI) with dsDNA causes breaking of hydrogen bonds, conformational changes, and unfolding of the double helix, which enables easier access of other oxidative agents to interact with DNA, and the occurrence of oxidative damage to DNA.

Keywords Chromium · Chromium intermediates–DNA interaction · DNA damage · Oxidative damage · Milli-8-Oxoguanine · Differential pulse voltammetry · Glassy carbon

S. C. B. Oliveira · A. M. Oliveira-Brett (✉)
Departamento de Química, Faculdade de Ciências e Tecnologia,
Universidade de Coimbra,
3004-535 Coimbra, Portugal
e-mail: brett@ci.uc.pt

Introduction

In recent years increased attention has been focused on the ways in which transition metal ions interact with double-stranded DNA (dsDNA), with the goal of understanding the toxic effects of some transition metal ions used in chemotherapy as well as in the development of novel metal-chelate chemotherapeutics.

Transition or d-block metals have the d-orbitals partially filled, and consequently, they can be regarded as having free radical behavior. Transition metals interact with more than two different sites, and their interactions with dsDNA are complicated. The positively charged metal ions interact directly or indirectly with sites characterized by high electron density or negatively charged residues of dsDNA. Such sites on dsDNA could be the negatively charged phosphates of the backbone of both strands and the electron donor atoms of the bases, such as N and O. The predominant mode of transition metal ion binding takes place at the N7 and O6 of guanine, the N7 and N1 of adenine bases, and the N3 of pyrimidines [1].

Among the transition metal ions, chromium occupies a unique position in biological studies. Of the various oxidation states of chromium, Cr(VI) exists as an oxyanion, which is structurally similar to phosphate and sulfate anion and may enter the cells through anion channel, leading to rapid intracellular accumulation [2–4]. This, in turn, has been found to be toxic due to the formation of reactive intermediate species, such as Cr(IV) and Cr(V), and reactive oxygen species (ROS) by the cellular reductants, such as ascorbate and glutathione [3, 5–14].

Any of these chromium-reactive intermediate species or radical species may potentially target dsDNA and cause various types of damage. It is described that Cr(V) has been implicated as the intermediate species responsible for direct

formation of a chromium–DNA adduct in vitro and *in vivo* [3, 5, 9–12]. In vitro, Cr(VI) has been shown to react with ascorbate to generate Cr(V) that causes chromium–DNA binding and DNA strand breaks [5]. Reactions of dsDNA with Cr(VI) in the presence of thiols led to the formation of the reactive intermediate Cr(V) and a chromium–DNA adduct, and the levels of chromium bound to dsDNA correlated with the levels and stability of the Cr(V) intermediate formed [15]. Between DNA bases, guanine has been found to be most vulnerable to oxidation by chromium species [9, 16–18]. However, consensus over the direct interaction between DNA and chromium species is still needed.

Electrochemical techniques, such as pulse techniques, are suitable for studies of biological systems, for instance dsDNA–metal ion interactions [19, 20], since they are fast, low cost, and have high sensitivity. One advantage of the use of pulse techniques is that they bring a great improvement in signal-to-noise ratio compared to steady-state techniques and, in many cases, greater selectivity [21]. Differential pulse voltammetry has been successfully utilized to investigate the interaction of small molecules with DNA and is a powerful tool in elucidating the nature of DNA–metal ion binding and in detecting the conformational changes and DNA oxidative damage. The oxidation products of guanine, 8-oxoguanine (8-oxoGua), and of adenine, 2,8-dihydroxyadenine (2,8-oxoAde), are biomarkers of DNA oxidative damage [22, 23]. These oxidation products, 8-oxoGua and 2,8-oxoAde, assemble, during DNA replication, pairing with the wrong pyrimidine base, cytosine or thymine, being considered natural cause of mutagenesis. The electrochemical oxidation peaks of the DNA components, nucleotides, nucleosides, purine, and pyrimidine bases [24, 25], are employed as the biological recognition signal for the determination of DNA specific interaction.

Among the electrochemical transducers, carbon electrodes demonstrate several unique properties. The extensive potential window in the positive direction allows sensitive electrochemical detection of the oxidative damage caused to DNA by monitoring the appearance of the oxidation peaks of the DNA bases. Chromium species were investigated using gold and platinum electrodes [26, 27]; however, no report has been published on the oxidation of Cr(III) using a glassy carbon electrode (GCE).

In the present paper, a systematic study has been undertaken to elucidate the mechanism of interaction of chromium species with dsDNA in aqueous solution, using differential pulse voltammetry at a GCE. The electrochemical oxidation signal of DNA purine base homopolynucleotides was employed for the biological recognition for the detection of preferential DNA base interaction.

Experimental

Materials and reagents

The sodium salt of highly polymerized calf thymus dsDNA (length, 10,000–15,000 bp), polyguanylic acid-poly[G] (length, 200–600 bp), polyadenylic acid-poly[A] (length, ~200 bp; from Sigma–Aldrich), and chromium (III) chloride and potassium chromate (from Merck) were used without further purification.

Solutions of 2.5 mM Cr(III) and 0.5 mM CrO_4^{2-} were prepared directly in pH 4.5 0.2-M acetate buffer-supporting electrolyte. A solution of 2.5 mM Cr(III) was also prepared directly in pH 4.5 0.2-M acetate buffer and stocked for 1 month before use and utilized as a source solution Cr(VI), since in these experimental conditions, Cr(III) in solution was oxidized to CrO_4^{2-} by the dissolved O_2.

Stock solutions of 300 μg mL^{-1} dsDNA, poly[G], and poly[A] were prepared in deionized water and kept at 4 °C. The solutions were diluted to the desired concentration by mixing buffer-supporting electrolyte. All solutions were prepared using analytical grade reagents and purified water from a Millipore Milli-Q system (conductivity ≤0.1 μS cm^{-1}).

In some experiments, the sample solutions were deoxygenated bubbling high purity N_2 in the sample solutions during the incubation period and continuing with a flow of pure N_2 over the solution during the voltammetric experiments.

Microvolumes were measured using EP-10 and EP-100 Plus Motorized Microliter Pippettes (Rainin Instrument Co. Inc., Woburn, USA). The pH measurements were carried out using a Crison micro-pH 2001 pH-meter with an Ingold combined glass electrode. All experiments were done at room temperature (25±1 °C).

UV–Vis absorption

Absorption spectra were recorded using a UV–Vis spectrophotometer SPECORD S100 from Carl Zeiss Technology with Win-Aspect software. The experimental conditions for absorption spectra were integration time 25 ms and accumulation 1,000 points. All UV–Vis spectra were measured from 300 to 800 nm.

Voltammetric parameters and electrochemical cells

Voltammetric experiments were carried out using a μAutolab running with GPES 4.9 software, Metrohm/Autolab, Utrecht, The Netherlands. The experimental conditions for cyclic voltammetry (CV) were scan rate 100 and 250 mV s^{-1}, and for differential pulse (DP) voltammetry, pulse amplitude 50 mV, pulse width 70 ms, and scan rate

5 mV s^{-1}. Measurements were carried out using a GCE (d=1.5 mm), with a Pt wire counter electrode and an Ag/AgCl (3 M KCl) electrode as reference, in a 0.5-mL one-compartment electrochemical cell.

The GCE was polished using diamond spray (particle size 1 μm) before every electrochemical assay. After polishing, the electrode was rinsed thoroughly with Milli-Q water. Following this mechanical treatment, the GCE was placed in buffer-supporting electrolyte, and various DP voltammograms were recorded until a steady-state baseline voltammogram was obtained. This procedure ensured very reproducible experimental results.

Acquisition and presentation of voltammetric data

All the voltammograms presented were background-subtracted and baseline-corrected using the moving average application with a step window of 5 mV included in GPES version 4.9 software. This mathematical treatment improves the visualization and identification of peaks over the baseline without introducing any artifact, although the peak intensity is in some cases reduced (<10%) relative to that of the untreated curve. Nevertheless, this mathematical treatment of the original voltammograms was used in the presentation of all experimental voltammograms for a better and clearer identification of the peaks. The values for peak current presented in all plots were determined from the original untreated voltammograms after subtraction of the base line.

Samples preparation

Cr-dsDNA, Cr-poly[G], and Cr-poly[A] were prepared by incubation at room temperature of 100 μg mL^{-1} dsDNA, poly[G], or poly[A] in pH 4.5 0.1-M acetate buffer with different concentrations of the desired chromium solution, during different periods of time: 10 min, 1 h, 6 h, 12 h, 24 h, and 60 h. Control solutions of dsDNA, poly[G], and poly[A] in pH 4.5 0.1-M acetate buffer were also prepared and stored during the same periods of time in similar conditions as the Cr-dsDNA-, Cr-poly[G]-, and Cr-poly[A]-incubated solutions. Incubations were also performed under N_2 deoxygenated conditions.

Results and discussion

The Pourbaix diagram for chromium [28, 29] shows that in solutions of pH between 1 and 6, Cr(VI) is present only in the form of $HCrO_4^-$, whereas Cr(III) occurs as Cr(III) ions and in the form of $CrOH_{aq}^{2+}$. At pH 4 to 6, the distribution of Cr(III) and Cr(VI) oxidation states is governed by the reaction below:

$$CrOH_{aq}^{2+} + 3H_2O \leftrightarrow HCrO_4^- + 6H^+ + 3e \quad (1)$$

with the possibility of O_2 being the electron acceptor. Furthermore, the intermediate species can occur as product of three consecutive Cr(III) one-electron step oxidations, Cr(III) to Cr(IV) to Cr(V) to Cr(VI).

The oxidation of Cr(III) by the O_2 dissolved in pH 4.5 0.1-M acetate buffer was investigated by CV and spectrophotometry (Figs. 1 and 2). This was very important to ascertain the presence of chromium-reactive intermediate species and clarify the evidence of each specie interaction with dsDNA.

UV–Vis absorption of chromium species

In order to verify that Cr(III) was oxidized to Cr(VI) by the O_2 dissolved in pH 4.5 0.1-M acetate buffer in the absence of other oxidants, the changes in the Cr(III) visible absorption spectrum were monitored with time. The absorption spectra of aqueous solutions of 2.5 mM Cr(III) and 0.5 mM CrO_4^{2-}, prepared in pH 4.5 0.1-M acetate buffer, are shown in Fig. 1. The wavelengths of maximum adsorption found for Cr(VI) are 350 and 442 nm, while for Cr(III), are 432 and 615 nm.

A solution of Cr(III) prepared in pH 4.5 0.1-M acetate buffer showed, after 60 h, two maximum absorbance peaks at 418 and 570 nm (Fig. 1), indicating that interaction between Cr(III) and dissolved O_2 occurred in a time-dependent manner. The redox reaction of Cr(III) into Cr(VI), or vice versa, can only take place in the presence of another couple which accepts or gives the three necessary electrons as already discussed above (Eq. 1), and in the experimental conditions used, the redox couple was $O_2/H_2O_{(aq)}$. Consequently, in an environment with dissolved O_2, there is an equilibrium between Cr(III)/Cr(VI), and chromium intermediate species will be present in solution. However, the UV–Vis technique suffers from poor selectivity and is not optimal

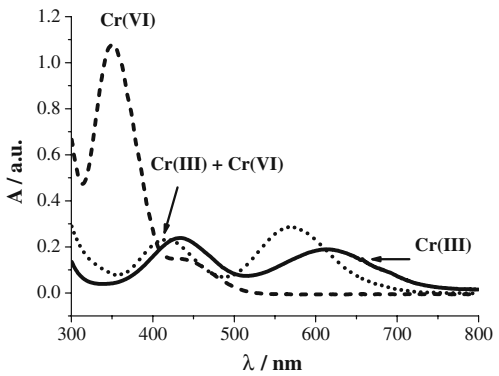

Fig. 1 Visible absorption spectra of aqueous, (*solid line*) 2.5 mM Cr (III), (*dashed line*) 0.5 mM Cr(VI), and (*dotted line*) 2.5 mM Cr(III), solution after 60 h preparation

for speciation analysis. So, these experiments were also done using electrochemical techniques.

Electrochemical behavior of chromium species

Chromium species are oxidizable at solid electrodes, and the redox behavior of the Cr(III)/Cr(VI) couple was studied by CV at a GCE in a solution of 2.5 mM Cr(III) in pH 4.5 0.1-M acetate buffer. The oxidation of Cr(III) by dissolved O_2 was investigated between −0.50 and +1.55 V, and four peaks were observed (Fig. 2a, b).

Successive cyclic voltammograms, in a freshly prepared solution of Cr(III), starting at an initial potential of 0.0 V, scanning in the positive direction to +1.55 V and after reversing the scan to the negative potential limit of −0.50 V, at scan rate ν=250 mV s^{-1}, presented four peaks (Fig. 2a). The oxidation of Cr(III) occurs by a multi-step mechanism where peak 1_a, at $E_{pa}{}^1$~+1.15 V, corresponds to the oxidation of Cr(III) to intermediate products Cr(IV)/Cr(V), peak 2_a, at $E_{pa}{}^2$~+1.40 V, is attributed to oxidation of Cr(V) to Cr(VI), and both reactions are irreversible. The Cr(VI) oxidation product of Cr(III) was reduced, giving rise to two reduction peaks, peak 3_c, at $E_{pc}{}^3$~−0.30 V, that corresponds to the reduction of Cr(VI) to Cr(V)/Cr(IV), and peak 4_c, at $E_{pc}{}^4$=−0.23 V, that corresponds to reduction of Cr(V) to Cr(III), and again, in both cases, the reactions were irreversible.

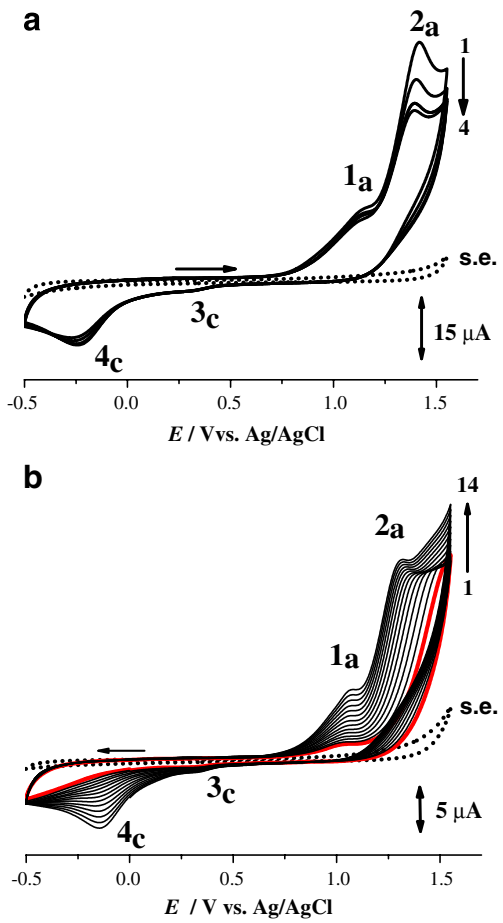

Fig. 2 Successive cyclic voltammograms in pH 4.5 0.1-M acetate buffer of 2.5 mM Cr(III): (**a**) freshly prepared solution, scan rate ν= 250 mV s^{-1} and (**b**) solution after 60 h, scan rate ν=100 mV s^{-1}; *red solid line*: first scan. *s.e.* supporting electrolyte

Cyclic voltammograms were obtained for different scan rates in a fresh solution of 2.5 mM Cr(III). Between measurements, the electrode surface was always polished in order to ensure a clean surface and to avoid possible problems from the adsorption of Cr(III) oxidation products onto the GCE surface. It was observed that, on increasing the scan rate, peak 2_a, at $E_{pa}{}^2$=+1.40 V, was slightly displaced to more positive values, confirming the irreversibility of the electrochemical reaction. Increasing the scan rate, the current of peak 2_a increases linearly with square root of ν, consistent with the diffusion-limited oxidation of a solution species. The difference between peak 2_a potential, $E_{pa}{}^2$, and the potential at peak half height, $E_{p/2a}{}^2$, is $|E_{pa}{}^2-E_{p/2a}{}^2|$~75 mV. Since for a diffusion-controlled irreversible system $|E_{pa}{}^2-E_{p/2a}{}^2|=47.7/(\alpha_a n')$, where α_a is the anodic charge transfer coefficient and n' is the number of electrons in the rate-determining step, it was calculated that $\alpha_a n'$=0.64, and since n'=1, for the peak 2_a irreversible reaction α_a=0.64 was found.

Due to the complexity of the chromium species redox process at the GCE surface, another experiment was performed after 60 h in a solution of 2.5 mM Cr(III) prepared in pH 4.5 0.1-M acetate buffer, using a clean GCE, and scanning between −0.50 V and a positive potential limit of +1.55 V, at scan rate ν=100 mV s^{-1}. No redox peaks were obtained in these conditions in the positive-going scan.

The experiment was repeated, but starting at an initial potential of 0.0 V, scanning in the negative direction until −0.50 V, and after reversing the scan to a positive potential limit of +1.55 V, at ν=100 mV s^{-1}, and successive scans were recorded. In the first scan in the negative direction, no well-defined cathodic peak appeared but, in the first scan in the positive direction, peak 1_a, at $E_{pa}{}^1$~+1.06 V (Fig. 2b) was already observed. In successive CV scans, the voltammograms revealed analogous electrochemical behavior to the experiments described above in a freshly prepared Cr(III) solution, and the peak 2_a, at $E_{pa}{}^2$~+1.30 V, the cathodic peak 3_c, at $E_{pc}{}^3$~−0.30 V, and the cathodic peak 4_c, at $E_{pc}{}^4$~−0.14 V, were clearly observed. This confirms that, for these experimental conditions, first the reduction of Cr(VI) to Cr(V)/Cr(IV) occurs, followed by the reduction to Cr(III), and afterwards re-oxidation of all the reduced chromium species.

The CVs clearly show that various chromium redox processes occur, and based on the results obtained, the peaks can be correlated with the different chromium oxidation states: peak 1_a to Cr(IV)/Cr(V), peak 2_a to Cr (VI), peak 3_c to Cr(V)/Cr(IV), and peak 4_c to Cr(III). These experiments confirm that Cr(III) was oxidized by the dissolved O_2, in a time-dependent manner, in pH 4.5 0.1-M acetate buffer at the concentration studied.

In situ evaluation of chromium species–DNA interaction

The knowledge of the kinetics and mechanism of the chromium species electrode processes enable the understanding of the dsDNA modifications after interaction with chromium species in solution.

The chromium species, Cr(III), Cr(IV), Cr(V), and Cr (VI), can cause a variety of DNA lesions, depending on the chromium oxidation state and the redox processes occurring upon their interaction with the genetic material. The ability of chromium species to induce hydrogen bonding cleavage, double helix deconformation, and/or oxidative damage to dsDNA was studied by DP voltammetry. In all experiments, different concentrations of Cr(III) and Cr(VI) were incubated for different periods of time with 100 μg mL^{-1} dsDNA, and their interaction was followed, using a GCE directly in solution, by the detection of the changes in dsDNA electrochemistry. The GCE surface was always cleaned between each measurement to avoid current decrease due to the strong adsorption of dsDNA after successive scans.

The oxidation behaviors of Cr(III), Cr(VI), poly[G], poly [A], and dsDNA, in pH 4.5 0.1-M acetate buffer using DP voltammetry between +0.2 and +1.4 V, are shown in Fig. 3, as they are the necessary controls to enable easier identification of the peaks occurring after the interactions

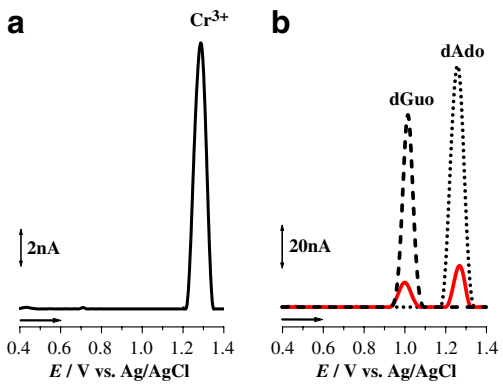

Fig. 3 Baseline-corrected DP voltammograms in pH 4.5 0.1-M acetate buffer: (**a**) 100 μM Cr(III) solution freshly prepared and (**b**) 100 μg mL^{-1}, dsDNA (*red solid line*), poly[G] (*black dashed line*), and poly[A] (*black dotted line*)

chromium species–DNA, chromium species–poly[G], and chromium species–poly[A].

In the DP voltammogram of 100 μM Cr(III) (Fig. 3a), only one oxidation peak occurs, at E_{pa}=+1.30 V, due to the two electron oxidation of Cr(III) to the intermediates Cr (IV)/Cr(V). In this experiment, the Cr(III) concentration was considerably decreased, and the peak potential was shifted in a positive direction [28]. As expected in a solution only with Cr(VI), no oxidation peak was observed.

The oxidation of 100 μg mL^{-1} dsDNA shows two small oxidation peaks (Fig. 3b), corresponding to the oxidation of desoxyguanosine (dGuo), at E_{pa}=+1.03 V [31], and desoxyadenosine (dAdo), at E_{pa}=+1.30 V [32], residues in the polynucleotide chain. The DP voltammogram of dsDNA shows two small oxidation peaks due to the difficulty of the electron transfer from the inside of the double-stranded rigid form of dsDNA to the electrode surface [33].

The DP voltammograms of the polyhomonucleotides, 100 μg mL^{-1} poly[G] and 100 μg mL^{-1} poly[A], show only one oxidation peak (Fig. 3b); poly[G] contains only guanine (Gua) residues and oxidation occurs at the desoxyguanosine (dGuo) residue, at E_{pa}=+1.03 V, while poly[A] contains only adenine residues and oxidation occurs at desoxyadenosine (dAdo), at E_{pa}=+1.30 V.

The effects of the chromium species–dsDNA interaction were followed by comparing the changes of the DNA oxidation peaks, desoxyguanosine (dGuo), and desoxyadenosine (dAdo) in the absence/presence of chromium species, and monitoring the appearance of the oxidation products of guanine (8-oxoGua) or/and adenine (2,8-oxoAde), which peaks both occur at E_{pa}=+0.45 V, vs. Ag/AgCl, in pH 4.5 0.1-M acetate buffer, and their occurrence is an indication of oxidative damage caused to DNA [34, 35]. A control solution of 100 μg mL^{-1} dsDNA was always prepared in acetate buffer and analyzed after the same periods of time as the Cr(III)–dsDNA- and Cr(VI)–dsDNA-incubated solutions.

The interaction between 100 μg mL^{-1} dsDNA and 100 μM Cr(III) was first studied after 10 min of incubation. The DP voltammogram, compared with the results from the control dsDNA solution, showed a small decrease of the oxidation peak current of dGuo, at E_{pa}=+1.03 V, and a large increase of the oxidation peak current of dAdo, at E_{pa}=+1.30 V (Fig. 4). The peak at E_{pa}=+1.30 V includes two contributions: the oxidation of dAdo residues and of Cr(III) ions, since both oxidations occur at exactly the same potential value (Fig. 3a, b). It was concluded, for the experimental conditions used, that there was no interaction between Cr(III) and dsDNA.

Cr(III)–dsDNA samples were investigated after 24 and 48 h incubation. The DP voltammogram of the sample incubated during 24 h showed a small difference from the

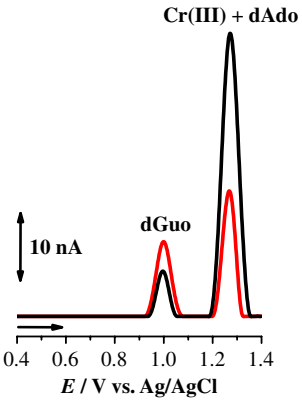

Fig. 4 Baseline-corrected DP voltammograms after 10 min incubation in pH 4.5 0.1-M acetate buffer of 100 μg mL^{-1} dsDNA: (*red solid line*) control and (*black solid line*) with ~100 μM Cr(III)

control dsDNA solution. Comparison with the results obtained after 10 min incubation showed a decrease of the oxidation peak current of dAdo, indicating a lower concentration of Cr(III), due to its partial oxidation by dissolved O_2, since the oxidation peak currents of dGuo and dAdo were unchanged. However, the DP voltammogram for 48 h incubation showed an increase of the oxidation peak currents of dGuo and dAdo due to the chromium–DNA interaction, compared with the results obtained in the dsDNA control solution.

The DP voltammogram obtained after 60 h dsDNA and Cr(III) incubation showed four well-defined oxidation peaks (Fig. 5). The oxidation peaks of dGuo and dAdo are observed, and they present an increase of the oxidation currents due to the chromium–DNA interaction, when compared with the results obtained in the dsDNA control solution. The oxidation peak found at E_{pa}=+0.45 V is attributed to 8-oxoGua and/or 2,8-oxoAde oxidation, and the peak observed at E_{pa}=+0.80 V is due to the oxidation of free guanine released from dsDNA after 60 h incubation.

Experiments were carried out for different incubation times, 5 min, 6 h, and 72 h, and 10 and 50 μM concentrations of Cr(III) and in N_2 deoxygenated samples. The increase in the oxidation peak current of dGuo and dAdo, and of the two new peaks observed, at E_{pa}=+0.45 V and E_{pa}=+0.80 V, was proportional to the increase of

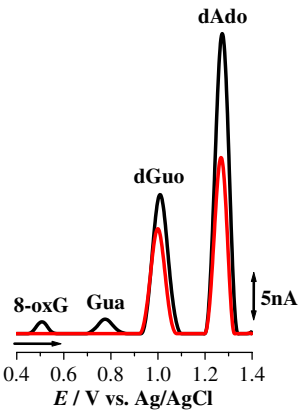

Fig. 5 Baseline-corrected DP voltammograms after 60 h incubation in pH 4.5 0.1-M acetate buffer of 100 μg mL^{-1} dsDNA: (*red solid line*) control and (*black solid line*) with ~100 μM Cr(III)

concentration and incubation time. However, in N_2 deoxygenated samples, without the presence of O_2, no detectable DNA oxidative damage was caused by Cr(III).

As already explained, the UV–Vis technique suffers from poor selectivity and sensitivity when compared with electrochemistry techniques, and is not optimal for these analyses. However, UV–Vis experiments were done for different incubation times, 5 min, 24 h, and 72 h, and 10, 50, and 100 μM concentrations of Cr(III), and for the experimental conditions before and after Cr(III)-DNA interaction, no difference was found.

The data obtained suggests that the Cr(III) intermediate oxidation products Cr(IV)/Cr(V) interact with dsDNA, leading to modifications in the double helical structure in a time-dependent manner without the involvement of any activated oxygenated species. As the double helix unwinds, the DNA bases are more exposed to the electrode surface thus facilitating their oxidation, which can explain the occurrence of higher oxidation peak currents for dGuo and dAdo with increasing incubation time. Evidence for a specific interaction between the dGuo residues and the chromium species are based on the appearance of the free guanine oxidation peak, at E_{pa}=+0.80 V. The guanine oxidation peak can be explained considering the oxidation of the C1′ carbon of deoxyribose [36] by Cr(IV)/Cr(V), that causes the liberation of bases.

The oxidative damage caused to DNA bases by chromium species was also detected electrochemically by monitoring the appearance of the bases oxidation product peak, which will be identified in the following experiments as 8-oxoGua, at E_{pa}=+0.45 V, in pH 4.5 0.1-M acetate buffer.

The above experiments were repeated using Cr(VI) incubated with dsDNA for different incubation times in order to investigate if Cr(VI) induced hydrogen bonding cleavage and/or oxidative damage to dsDNA. The interaction between 100 μg mL^{-1} dsDNA and ~100 μM Cr(VI) was first studied after 1 h of incubation. The DP voltammogram showed an increase of the oxidation peak current for dGuo and dAdo compared with the results obtained in the control dsDNA solution. In other experiments, Cr(VI) was incubated with dsDNA for 24 and 60 h, and in both cases, the results show an increase of the oxidation peak current for dGuo and dAdo, and a new peak from free guanine, at E_{pa}=+0.80 V, compared with the results obtained for the control dsDNA solution (Fig. 6).

Experiments were carried out for different incubation times and concentrations of Cr(VI). The increase in current of the dGuo and dAdo oxidation peaks and of the peak observed from guanine, at E_{pa}=+0.80 V, was proportional to the increase of concentration and incubation time.

The damage caused by Cr(VI) to DNA was detected electrochemically by the oxidation peak current increase for

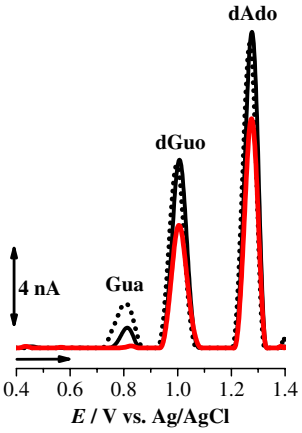

Fig. 6 Baseline-corrected DP voltammograms in pH 4.5 0.1-M acetate buffer of 100 μg mL^{-1} dsDNA: (*red solid line*) control and incubated with ~100 μM Cr(VI) during (*black solid line*) 24 h and (*black dotted line*) 60 h

dGuo and dAdo and the appearance of the oxidation peak for free guanine, at E_{pa}=+0.80 V, only after long time, 24 and 60 h, of Cr(VI) incubation with dsDNA. This is due to breaking of the hydrogen bonds and subsequent oxidation of the C1′ carbon of deoxyribose [36], which causes the liberation of bases enabling the oxidation of guanine on the GCE surface.

The direct interaction Cr(VI)–DNA occurred in the absence of ROS considering that first, this interaction occurs *in situ* and in the absence of Cr(VI) cellular reductants such as H_2O_2, ascorbate, and glutathione; second, Cr(VI) is strongly oxidizing; and third, the dsDNA protonation in acetate buffer neutralizes, in part, the phosphate groups and increases their interaction with the negatively charged Cr(VI) species.

In situ evaluation of chromium species–poly[G] and poly[A] interaction

In order to obtain more information about the preferential interaction of chromium species with dsDNA, experiments were performed using 100-μM Cr(III) solutions incubated with polynucleotides of known sequences, namely, poly[G] and poly[A], after 60 h incubation, as described in the "Sample preparation" section.

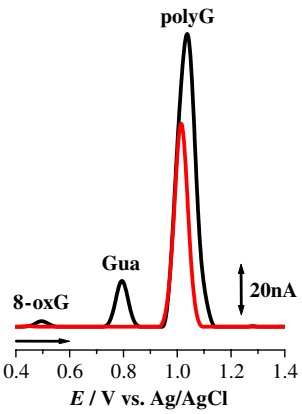

Fig. 7 Baseline-corrected DP voltammograms after 60 h incubation in pH 4.5 0.1-M acetate buffer of 100 μg mL^{-1} polyG: (*red solid line*) control and (*black solid line*) with ~100 μM Cr(III)

The DP voltammogram obtained for the Cr(III)–poly[A]-incubated sample showed only a very small decrease in dAdo oxidation peak current, when compared with the results obtained for the control poly[A] solution, and no oxidation peaks were found at E_{pa}=+0.45 V and at E_{pa}=+0.80 V. This indicates that the interaction of Cr(III) with the adenine base was negligible.

On the other hand, the DP voltammogram obtained for the Cr(III)–poly[G]-incubated sample, when compared with the results from the control poly[G] solution (Fig. 7), showed an increase of the signals corresponding to dGuo oxidation, and the appearance of the two new peaks for 8-oxoGua, at E_{pa}=+0.45 V, and for guanine, at E_{pa}=+0.80 V, indicating that oxidative damage had occurred in the poly[G] after 60 h incubation. The dGuo peak current increase can be explained considering conformational changes, by the unwinding of the quadruple and/or double helix structure of poly[G] in acid media, pH 4.5 [17], thus exposing the guanine bases for oxidation. On the other hand, the guanine release from poly[G] structure can be explained considering the oxidation of the C1′ carbon of deoxyribose [36], that causes the liberation of bases.

The experiments using poly[G] and poly[A] added new information to the understanding of the molecular mechanism involved in chromium species–DNA interaction. The preferential interaction with poly[G], and the occurrence of DNA oxidative damage, was clearly shown by the appearance of the oxidation peak of 8-oxoGua, at E_{pa}=+0.45 V, due to the oxidation of the guanine residues by the more toxic chromium higher oxidation state reactive intermediate species.

Chromium species–DNA damage

All the above results concerning the Cr(III)-DNA interaction are very important and have to be analyzed considering also the redox reaction mentioned earlier between the Cr(III) and solution dissolved O_2, in the experimental conditions investigated here.

First, the redox reactions between the Cr(III) and dissolved O_2 lead to the formation of more toxic chromium-reactive intermediate species. Second, the different chromium oxidation state species responsible as a precursor for the occurrence of DNA oxidative damage should be identified. Third, the oxidation potential for the interaction of these different chromium oxidation state species with dsDNA should be determined.

As shown in the "Electrochemical behavior of chromium species" section, a solution of Cr(III) in pH 4.5 0.1-M acetate buffer is oxidized by dissolved O_2, and the intermediates are the product of the consecutive one-electron Cr(III) oxidation to Cr(IV) to Cr(V) to Cr(VI).

Based on the higher reactivity of the intermediates of Cr(III) oxidation and that DNA oxidative damage was only observed after a long incubation time of 60 h, the results obtained show that the DNA damage observed concerning the Cr(III)-DNA interaction was not due to direct Cr(III) interaction with dsDNA but was due to interaction with the oxidized reactive intermediates, i.e., Cr(IV)–dsDNA and Cr(V)–dsDNA, formed during Cr(III) oxidation to Cr(VI) with time by dissolved O_2. Also, the absence of DNA oxidative damage in solution up to 24 h is in agreement with the slow oxidation of Cr(III) to Cr(VI) by dissolved O_2. Oxidative damage caused by Cr(III) to DNA was detected electrochemically by the oxidation peak current increase for dGuo and dAdo, and the appearance of the oxidation peaks for guanine and 8-oxoGua, only after a long time of Cr(III) incubation with dsDNA.

The damage caused by Cr(VI) to DNA was detected electrochemically by the oxidation peak current increase for dGuo and dAdo and the appearance of the oxidation peak for free guanine, only after long time, of Cr(VI) incubation with dsDNA. This is due to breaking of the hydrogen bonds and the unfolding of the double helix structure of dsDNA enabling the oxidation of guanine on the GCE surface, but this interaction did not lead to appearance of 8-oxoGua, the guanine oxidation product. However, the dsDNA conformation changes detected expose the DNA bases to the action of other oxidative agents.

The results showed direct evidence of the interactions between different chromium species and DNA in acidic media at pH 4.5, and considering that first, at pH 4.5, the dsDNA structure is in the B-form [33]; second, DNA oxidation is pH dependent; and third, the oxidation process is more difficult in acidic media; it can be concluded that these oxidation processes can also occur at physiological pH.

Conclusions

The study of the interaction of dsDNA with the chromium species Cr(III), Cr(IV), Cr(V), and Cr(VI), using DP voltammetry, clarifies the mechanism by which different chromium species bind to dsDNA causing their mutagenic action. The different interactions with dsDNA of the reactive intermediates of Cr(III) oxidation by the dissolved O_2 in solution causing DNA oxidative damage, and of Cr(VI) leading to conformational modifications of the dsDNA double helix, were described.

The Cr(IV) and Cr(V) intermediates were produced in situ through Cr(III) oxidation by O_2 dissolved in the solution. On the other hand, *in vivo* Cr(VI) reduction by ascorbate and glutathione will also produce Cr(IV) and Cr(V) intermediates and, finally, Cr(III). However, independently of Cr(III) oxidation or Cr(VI) reduction, the chromium species–DNA interaction, Cr(III)–DNA, Cr(IV)–DNA, Cr(V)–DNA, and Cr(VI)–DNA, will be the same. The procedure used enabled, as described, the separate investigation of the interaction and toxicity of each chromium species with DNA.

Using polynucleotides of known sequences, it was confirmed that chromium intermediates preferentially interact with dsDNA at guanine-rich segments, leading to oxidative damage and formation of the 8-oxoGua, guanine oxidation product. These results enabled a better understanding of the molecular mechanisms involved in chromium species-induced neoplasia.

The sensitivity of electrochemical pulse techniques offers the possibility to follow the interaction of metal ions with DNA under different conditions. However, it is evident that a correlation between electrochemical results and data obtained by means of other methods, especially in vivo methods, is necessary.

Acknowledgements Financial support from Fundação para a Ciência e Tecnologia (FCT), Ph.D. Grant SFRH/BD/27322/2006 (S.C.B. Oliveira), projects PTDC/QUI/65732/2006 and PTDC/QUI/098562/2008, POCI (co-financed by the European Community Fund FEDER), and CEMUC-R (Research Unit 285) is gratefully acknowledged.

References

1. Anastassopoulou J (2003) J Mol Struct 651:19–26
2. O'Brien TJ, Ceryak S, Patierno SR (2003) Mutat Res 533:3–36
3. Yuann JMP, Liu KJ, Hamilton JW, Wetterhahn KE (1999) Carcinogenesis 20:1267–1275
4. Vaidyanathan VG, Weyhermuller T, Nair BU, Subramanian J (2005) J Inorg Biochem 99:2248–2255
5. Stearns DM, Kennedy LJ, Courtney KD, Giangrande PH, Phieffer LS, Wetterhahn KE (1995) Biochemistry 34:910–919
6. Bose RN, Fonkeng BS, Moghaddas S, Stroup D (1998) Nucleic Acids Res 26:1588–1596
7. Bose RN, Moghaddas S, Mazzer PA, Dudones LP, Joudah L, Stroup D (1999) Nucleic Acids Res 27:2219–2226
8. Joudah L, Moghaddas S, Bose RN (2002) Chem Commun 16:1742–1743
9. Sugden KD, Martin BD (2002) Environ Health Perspect 110:725–728
10. Sugden KD, Rigby KM, Martin BD (2004) Toxicol in Vitro 18:741–748
11. Mazzer PA, Maurmann L, Bose RN (2007) J Inorg Biochem 101:44–55
12. Vacek J, Mozga T, Cahova K, Pivonkova H, Fojta M (2007) Electroanalysis 19:2093–2102
13. Zhitkovich A (2005) Chem Res Toxicol 18:3–11
14. Casadevall M, Fresco PD, Kortenkamp A (1999) Chem Biol Interact 123:117–132
15. Borges KM, Boswell JS, Liebross RH, Wetterhahn KE (1991) Carcinogenesis 12:551–561
16. Dickman MH, Pope MT (1994) Chem Rev 94:569–584
17. Sugden KD, Campo CK, Martin BD (2001) Chem Res Toxicol 14:1315–1322

18. Wolf T, Kasemann R, Ottenwalder H (1989) Carcinogenesis 10:655–659
19. Oliveira SCB, Corduneanu O, Oliveira-Brett AM (2008) Bioelectrochemistry 72:53–58
20. Chiorcea-Paquim AM, Corduneanu O, Oliveira SCB, Diculescu VC, Oliveira-Brett AM (2009) Electrochim Acta 54: 1978–1985
21. Brett CMA, Oliveira-Brett AM (2003) In: Bard AJ, Stratmann M (eds) Encyclopedia of electrochemistry. Wiley-VCH Verlag, Weinheim
22. Oliveira-Brett AM, Diculescu V, Chiorcea-Paquim AM, Serrano SHP (2007) In: Alegret S, Merkoçi A (eds) Comprehensive analytical chemistry. Elsevier, Amsterdam
23. Oliveira-Brett AM (2006) In: Grimes CA, Dickey EC, Pishko MV (eds) Encyclopedia of sensors. American Scientific Publishers, Stevenson Ranch, California
24. Paleček E, Fojta M, Jelen F, Vetterl V (2002) In: Bard AJ, Stratmann M (eds) The encyclopedia of electrochemistry. Wiley-VCH Verlag, Weinheim
25. Oliveira-Brett AM, Piedade JAP, Silva LA, Diculescu VC (2004) Anal Biochem 332:321–329
26. Welch CM, Hyde ME, Nekrassova O, Compton RG (2004) Phys Chem Chem Phys 6:3153–3159
27. Zanello P, Raspi G (1977) Anal Chim Acta 88:237–243
28. Ball JW, Nordstrom DK (1998) J Chem Eng Data 43:895–918
29. Richard FC, Bourg ACM (1991) Water Res 25:807–816
30. Kelsall GH, House CI, Gudyanga FP (1988) J Electroanal Chem 701 244:179–201
31. Oliveira-Brett AM, da Silva LA, Brett CMA (2002) Langmuir 18:2326–2330
32. Goyal RN, Sangal A (2002) J Electroanal Chem 521:72–80
33. Oliveira SCB, Oliveira-Brett AM (2010) Comb Chem High Throughput Screen 13:628–640
34. Oliveira-Brett AM, Piedade JAP, Serrano SHP (2000) Electrochemical oxidation of 8-oxoguanine. Electroanalysis 12:969–973
35. Diculescu VC, Piedade JAP, Oliveira-Brett AM (2007) Bioelectrochemistry 70:141–146
36. Rhaese HJ, Freese E (1968) Biochim Biophys Acta 155:476–490